AJNR

MR of esthesioneuroblastoma (olfactory neuroblastoma) and appearance after craniofacial resection.

J J Schuster, C D Phillips and P A Levine

AJNR Am J Neuroradiol 1994, 15 (6) 1169-1177
http://www.ajnr.org/content/15/6/1169

MR of Esthesioneuroblastoma (Olfactory Neuroblastoma) and Appearance after Craniofacial Resection

James J. Schuster, C. Douglas Phillips, and Paul A. Levine

PURPOSE: To analyze the MR characteristics of a series of patients with esthesioneuroblastoma and discuss the typical surgery and its postoperative MR appearance. **METHODS:** The MR studies of 15 patients with the pathologic diagnosis of esthesioneuroblastoma (also known as olfactory neuroblastoma) were retrospectively reviewed and correlated with CT and surgical findings. The postoperative MR studies of 10 patients who underwent craniofacial resection were also reviewed. **RESULTS:** In all cases the tumors arose in the superior nasal cavity and extended into the ethmoid cells. In some instances the tumors extended into the other paranasal sinuses, orbits, anterior cranial fossa, and cavernous sinus. The tumors were typically expansile and destructive in their growth patterns. Compared with brain gray matter, the tumors were hypointense on T1-weighted images and isointense to hyperintense on T2-weighted images. Nine tumors were heterogeneous and 6 were homogeneous. Contrast enhancement ranged from mild to marked. MR was useful for characterizing the various tissues and distinguishing fluid in the postoperative nasal cavity. **CONCLUSIONS:** Esthesioneuroblastoma, although an uncommon tumor, may be suspected in lesions of the superior nasal cavity demonstrating both expansile and destructive growth properties. The MR findings are otherwise nonspecific. MR is the imaging modality of choice for depicting local tumor extension and evaluating for recurrence after craniofacial resection.

Index terms: Esthesioneuroblastoma; Nasal cavity; Paranasal sinuses, neoplasms; Head, magnetic resonance

AJNR Am J Neuroradiol 15:1169–1177, Jun 1994

Esthesioneuroblastoma, also referred to as olfactory neuroblastoma, is an uncommon malignant tumor of neural crest origin that arises from the olfactory epithelium of the superior nasal cavity. High-resolution computed tomography (CT) has been the imaging procedure of choice. In our experience, magnetic resonance (MR) can provide additional information that is crucial for treatment planning because the tumor is often more extensive than clinically appreciated. The treatment policy at our institution consists of preoperative radiotherapy preceding craniofacial resection. Adjuvant chemotherapy is reserved for tumor spread beyond the nasal cavity and paranasal sinuses. Craniofacial resection uses a frontal craniotomy to permit a safe, controlled resection of the cribriform plate and fovea ethmoidalis region.

Materials and Methods

We retrospectively reviewed the MR studies of 15 patients referred to our institution with esthesioneuroblastoma. The pathologic reports of all 15 patients and the surgical, hospital, and outpatient records of all but two patients were available for review. These clinical data were correlated with the MR findings. The patients ranged in age from 16 to 73 years (mean, 53 years); 10 were male and 5 female. MR examinations were performed at initial tumor presentation in 11 patients. Four patients had MR exams that demonstrated tumor recurrence after previous surgery (2 after lateral rhinotomy and 2 after craniofacial resection). Nine of these patients were reimaged after preoperative adjuvant therapy (ie, radiation alone or chemotherapy plus radiation). Eight patients with esthesioneuroblastoma were imaged at 1.5 T (Siemens Magnetom, Iselin, NJ, 7 patients; General Electric Signa, Milwaukee, Wis, 1 patient), 4 at 1.0

Received May 4, 1993; accepted pending revision August 12; revision received September 9.

From the Departments of Radiology (J.J.S., C.D.P.) and Otolaryngology (P.A.L.), University of Virginia Health Sciences Center, Charlottesville.

Address reprint requests to C. Douglas Phillips, MD, Department of Radiology, Box 170, University of Virginia Health Sciences Center, Charlottesville, VA 22908.

AJNR 15:1169–1177, Jun 1994 0195-6108/94/1506–1169

T (Siemens Magnetom), 1 at 0.5 T (Picker Vista Q, Highland Heights, Ohio), and 2 at 0.3 T (Beta 3000 M, Fonar, Melville, NY).

Spin-echo images acquired had 3- to 5-mm thickness, 256 × 256 or 256 × 192 matrix, and 18- to 23-cm field of view. Consecutive sections were separated by a 1.0- or 2.5-mm gap. T1-weighted images (500–800/20–25/2 [repetition time/echo time/excitations]) and T2-weighted images (2200–2500/20–30, 60–90/1) were obtained in all patients. Sagittal T1-weighted images were acquired in all 15 patients with esthesioneuroblastoma. Images were acquired in the coronal plane in 14 examinations (T1-weighted images in 12 patients, T2-weighted images in 12 patients). Images were acquired in the axial plane in 14 examinations (T1-weighted images in 6, T2-weighted images in 8). Images were enhanced with gadopentetate dimeglumine (Magnevist, Berlex Laboratories, Cedar Knolls, NJ) in 10 patients (coronal plane in 10 patients, sagittal plane in 7, axial plane in 4); in the other 5 patients the scans predated its availability. Eleven patients with esthesioneuroblastoma also had coronal CT exams (6 patients, Siemens DRH; 4 patients, GE 9800; 1 patient, Picker PQ 2000).

MR images of patients with esthesioneuroblastoma were retrospectively reviewed by two of us (J.J.S. and C.D.P.). We compared the tumor signal characteristics on all sequences to brain gray matter. MR and CT images were compared to determine their ability to depict tumor extension, bone destruction, nasal cavity expansion, involvement of the cribriform plate, hemorrhage, calcification, and differentiation from entrapped sinus fluid. The imaging findings were correlated with surgical or biopsy findings in 13 patients.

Ten patients had MR results available for review after craniofacial resection. Eight of these had gadopentetate dimeglumine–enhanced T1-weighted scans; the studies in the two other patients predated contrast availability. All these studies were performed at our institution (Siemens 1.5 T, 9 patients; Siemens 1.0 T, 1 patient). Two of these patients also had postoperative CT results available for review.

Results

MR demonstrated that all 15 tumors were centered in the superior nasal cavities with extension into the ethmoid sinuses. Tumor extension into the following additional locations was demonstrated: maxillary sinus (9 patients), sphenoid sinus (2 patients), frontal sinus (2 patients), orbits (5 patients), anterior cranial fossa (6 patients), brain (1 patient), cavernous sinus (2 patients), and pterygomaxillary fossa (1 patient). These findings were confirmed in 13 patients by reviewing the surgical reports. Compared with brain gray matter, 10 tumors were hypointense and 5 isointense on T1-weighted images; 9 isointense, 5 hyperintense, and 1 hypointense on proton-density images; and 7 isointense and 8 hyperintense on T2-weighted images. Contrast enhancement was uniform in 6 of 10 tumors (Fig 1C) and heterogeneous in 4 of 10 tumors (Figs 2, 3, and 4). The enhancement ranged from mild to marked.

MR clearly was superior to CT in differentiating tumor from entrapped sinus fluid. Coronal images generally yielded the most useful information. In most cases, the T2-weighted images were excellent in demonstrating the contrast between very high signal sinus fluid and moderately high to intermediate signal intensity of tumor (Fig 1C). However, there were three cases in which precontrast and postcontrast T1-weighted images were superior in making this distinction. This usually occurred when sinus fluid had an intermediate signal intensity on T2-weighted images that was similar to the tumor. In these cases, the tumor diffusely enhanced, whereas the fluid-filled sinuses demonstrated only peripheral mucosal enhancement (Figs 1D and 1E).

The tumor had homogeneous signal intensity on T2-weighted images and noncontrast T1-weighted images in 6 patients (Fig 1). In 9 patients the tumor had a heterogeneous MR appearance on postcontrast T1- and T2-weighted images (Fig 2). Four of the 6 tumors that extended into the anterior cranial fossa had heterogeneous signal. Two of the four tumor recurrences were heterogeneous (Fig 3). Signal heterogeneity was also helpful in distinguishing tumor from entrapped sinus fluid (Figs 2A and 2B). Calcification was demonstrated in 4 of the 11 patients who had preoperative CT examinations. One of these was a tumor recurrence. The MR examination of only one patient demonstrated foci of low signal that corresponded to calcifications on CT. Focal hemorrhage was not seen within any tumor, with the exception of patients who had undergone recent biopsy. Biopsy sites appeared as small foci of high signal on T1-weighted images, generally in the anterior inferior aspect of the tumor.

We characterized 12 of the 15 tumors as expansile and destructive. The tumors of two patients were thought to be purely destructive. The expansile tendency of esthesioneuroblastoma was characterized by bowing of the sinus walls (Figs 2–4). The destructive nature was manifested as tumor replacing the turbinates, nasal septum, and sinus walls with extension into contiguous areas (Fig 1). Another patient had a subtle tumor recurrence that was neither expansile nor destructive but was biopsied after MR demonstrated

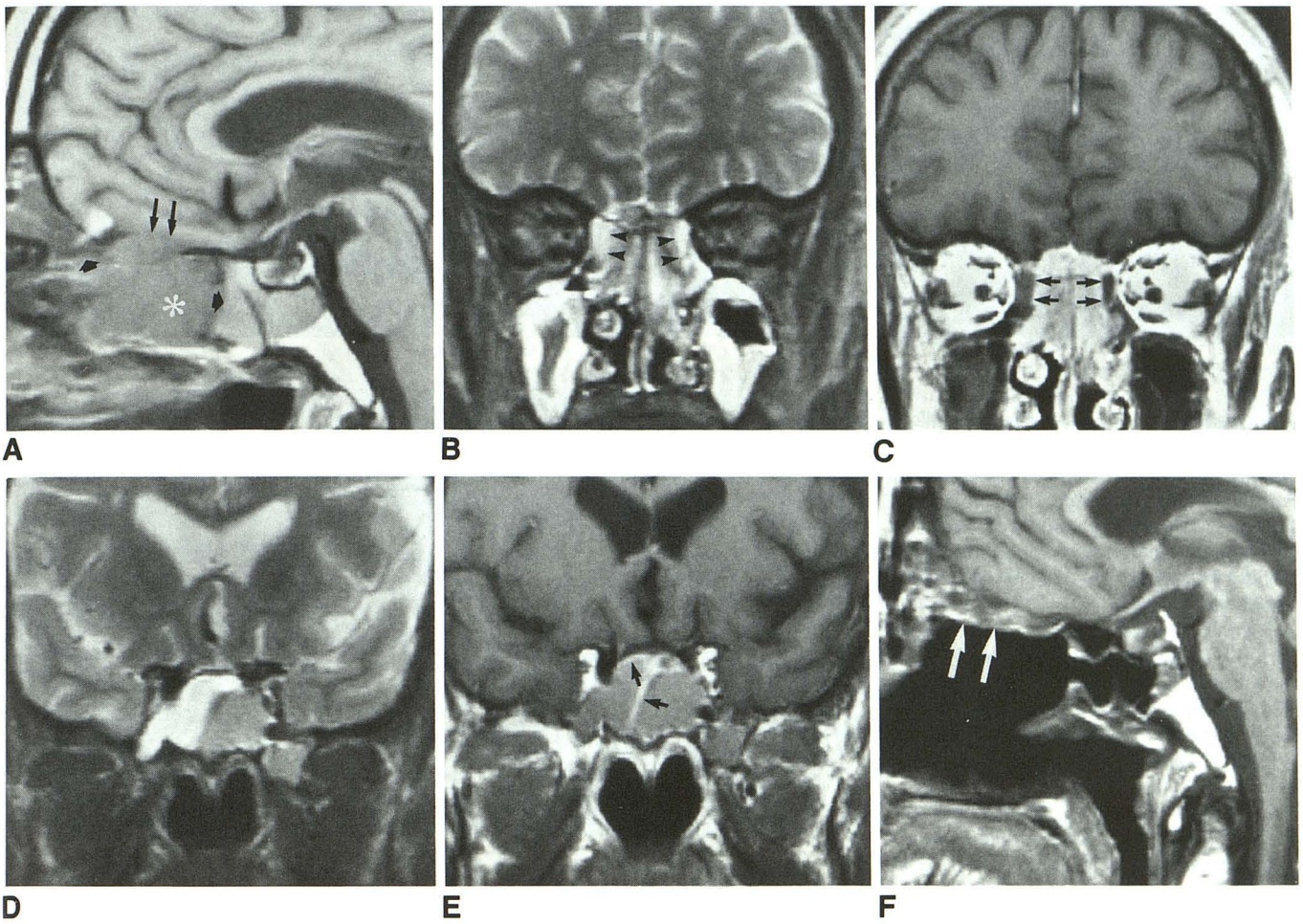

Fig. 1. Sixty-seven-year-old man with nasal stuffiness. *A* to *E* are from pretherapy MR study. *F* and *G* are from MR study 10 months after craniofacial resection.

A, Precontrast sagittal T1-weighted image shows a mass *(asterisk)* with homogeneous intermediate signal in the superior nasal cavity with extension through the cribriform plate. Because the usual linear low signal of dura was absent *(short arrows)*, the tumor was thought to have invaded through the dura into the anterior cranial fossa. This was confirmed at surgery. Tumor is differentiated from fluid in the frontal sinus and sphenoid sinus *(long arrows)* by different signal intensity.

B, Coronal T2-weighted image (2500/90) shows the mass to have homogeneous intermediate signal (isointense to gray matter). The mass is easily distinguished from fluid-filled ethmoid sinuses *(arrowheads)*.

C, Postcontrast coronal T1-weighted image (500/20), same level as *B,* shows a uniform, moderately enhancing mass that is distinguished from low-signal fluid in the uninvolved ethmoid sinuses *(arrows)*. The superior extent of the tumor is well depicted.

D, Coronal T2-weighted image shows high-signal inflammatory fluid in the right side of the sphenoid sinus and intermediate signal filling the left side of the sinus. On this image it cannot be determined whether the left side of the sinus contains fluid or tumor.

E, Postcontrast coronal T1-weighted image, at same location as *D,* demonstrates no tumor in the sphenoid sinus, only intermediate-signal inflammatory fluid. There is peripheral mucosal enhancement within the sinus *(arrowheads)*.

F, Precontrast sagittal T1-weighted image after craniofacial resection. Tumor mass has been removed, and there is tissue with mixed intermediate and high signal *(arrows)* in the superior nasal cavity and frontal sinus, which represents the fat, fascia, and muscle grafts placed at surgery (see text).

G, Postcontrast coronal T1-weighted image after craniofacial resection, at a location similar to *B* and *C,* shows uniform enhancing tissues in the superior nasal cavity *(arrow)*. This is a common postoperative finding, representing granulation tissue. The tumor, middle and superior turbinates, nasal septum, and ethmoid sinuses have been resected. There is inflammatory fluid with irregular mucosal enhancement within both maxillary sinuses.

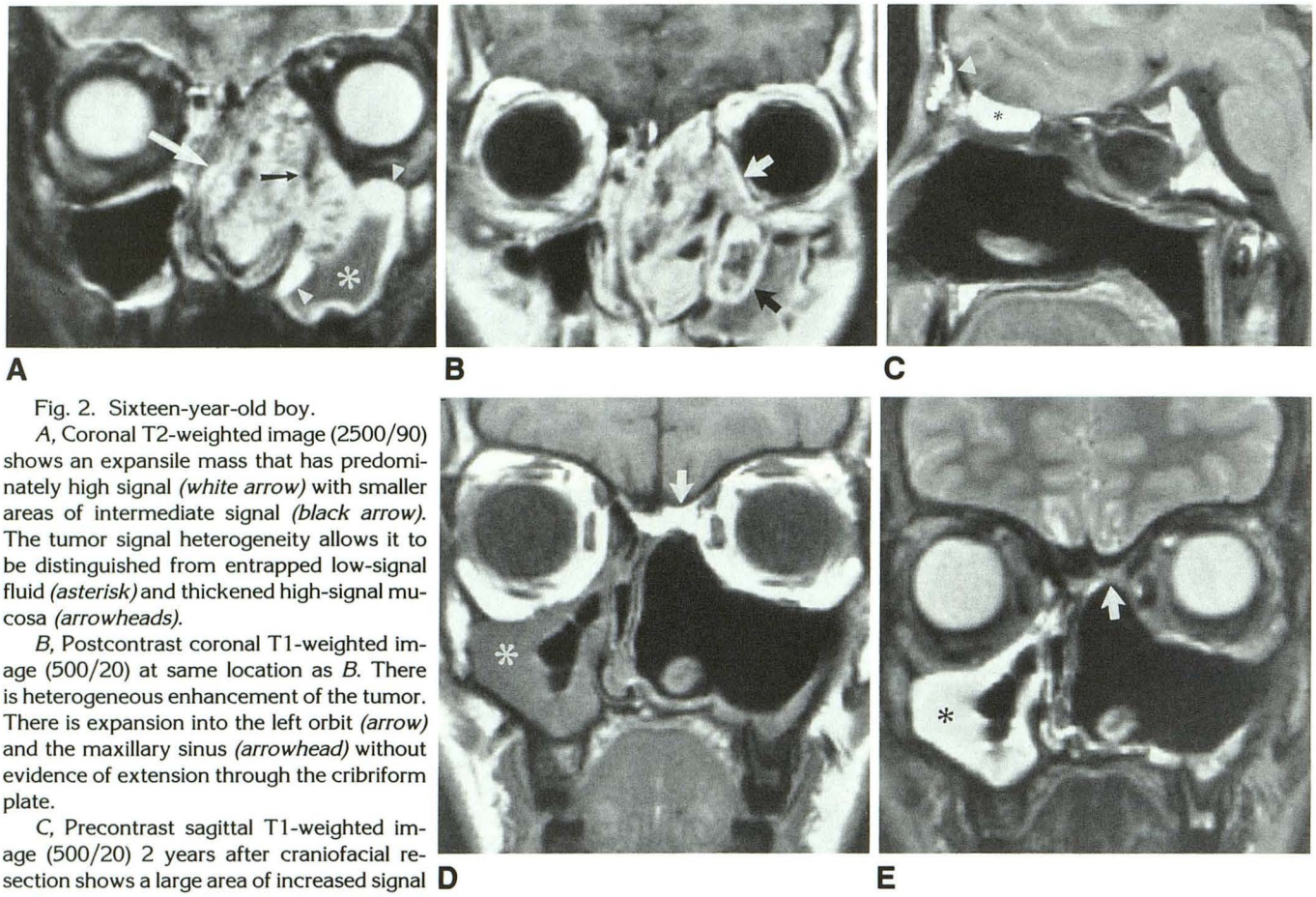

Fig. 2. Sixteen-year-old boy.

A, Coronal T2-weighted image (2500/90) shows an expansile mass that has predominately high signal *(white arrow)* with smaller areas of intermediate signal *(black arrow).* The tumor signal heterogeneity allows it to be distinguished from entrapped low-signal fluid *(asterisk)* and thickened high-signal mucosa *(arrowheads).*

B, Postcontrast coronal T1-weighted image (500/20) at same location as *B.* There is heterogeneous enhancement of the tumor. There is expansion into the left orbit *(arrow)* and the maxillary sinus *(arrowhead)* without evidence of extension through the cribriform plate.

C, Precontrast sagittal T1-weighted image (500/20) 2 years after craniofacial resection shows a large area of increased signal in the superior nasal cavity *(asterisk)* and in the region of the obliterated frontal sinus *(arrowhead).* This finding was unchanged when compared with an MR study 1 year after craniofacial resection (not shown) and represents fat placed at the time of surgery.

D and *E,* Coronal precontrast T1-weighted image (500/20) and T2-weighted image (2500/20) 2 years after craniofacial resection at similar locations as *B* and *C.* There has been resection of the tumor, superior and middle turbinates, left ethmoid sinuses, and the medial wall of the left maxillary sinus. Residual fluid is seen in the right maxillary sinus and remaining portions of the right ethmoid sinuses *(asterisks).* Tissue placed at surgery in the superior nasal cavity follows the signal characteristics of fat *(arrows).*

persistent soft tissue in the high nasal cavity. Both CT and MR were able to demonstrate orbital and intracranial involvement (anterior cranial fossa, cavernous sinus, and brain) in all patients subsequently shown to have tumor extension to these regions at surgery. We considered MR more accurate in depicting the exact margins of intracranial tumor extension because of its ability to obtain direct sagittal and coronal images and superior contrast between tumor and normal tissue, such as dura. In the one patient with brain invasion, the subarachnoid spread of tumor was seen only on MR (Fig 4). The cribriform plate seemed to be involved on MR in 11 of 15 patients and in 8 of 11 patients who had preoperative CT examinations. These data correlated with the findings at surgery. All 8 patients who had cribriform plate involvement on CT demonstrated this finding on MR.

There were two tumor recurrences in the 10 patients who had MR after craniofacial resection. We believe sagittal and coronal images best depicted the nasal cavities after tumor, turbinate, and cribriform plate removal. Noncontrast MR demonstrated varying amounts of soft tissue with a range of signal intensities in the superior nasal cavities. This depended on what type of tissue (muscle, fat, bone, fascia, or combinations thereof) was placed in this region after resection (Figs 2C–2E). Enhancing tissue usually persisted in the superior nasal cavity after craniofacial resection. This tissue ranged from 2 to 10 mm in thickness and was hypointense or hyperintense on T2-weighted images. In one of our patients this tissue was biopsied 6 months after craniofacial resection and at pathologic examination represented granulation tissue. Serial follow-up MR scans were useful in assessing for stability or

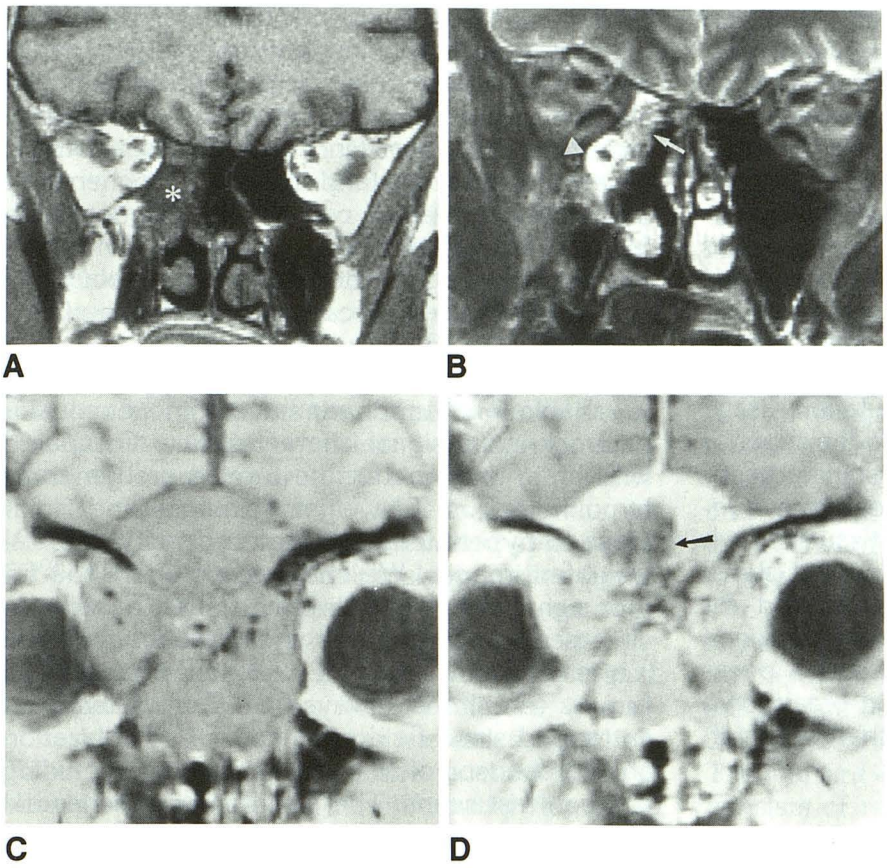

Fig. 3. Forty-three-year-old woman who underwent craniofacial resection in January 1988 for esthesioneuroblastoma. *A* and *B*, done in June 1988. *C* and *D*, done January 1990. MR studies performed in December 1988 and December 1989 (not shown) demonstrated increasing size of recurrent tumor.

A, Precontrast coronal T1-weighted image (500/20) shows low-signal tissue *(asterisk)* in the right superior nasal cavity that cannot be distinguished from entrapped fluid.

B, Coronal T2-weighted image (2500/90) shows intermediate signal in the right superior nasal cavity *(arrow)* that is distinguished from entrapped fluid *(arrowhead)*. The possibility of residual tumor was raised on this initial postoperative scan.

C and *D*, Coronal T1-weighted images (500/20) before and after contrast administration show huge expansile tumor recurrence with spread into both orbits and anterior cranial fossa. The central area of nonenhancement presumably represents necrosis *(arrow)*.

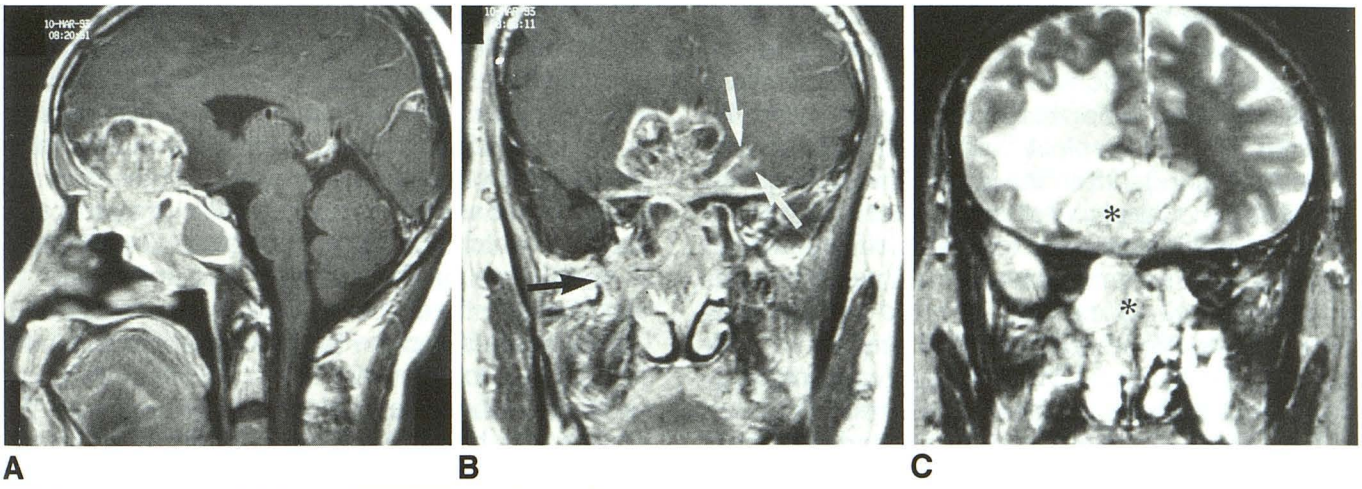

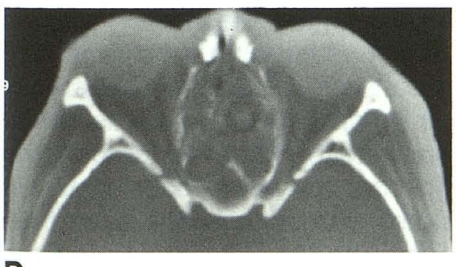

Fig. 4. Forty-seven-year-old woman.

A and *B*, Postcontrast sagittal and coronal T1-weighted images show an expansile mass with heterogeneous enhancement that extends from the superior nasal cavity superiorly into the anterior cranial fossa. Irregular linear enhancement between sulci indicates subarachnoid spread of the tumor *(white arrows)*. Entrapped sphenoid sinus fluid has low signal with peripheral mucosal enhancement. The enhancing tumor also extends into the right pterygomaxillary fossa *(black arrow)*.

C, Coronal T2-weighted image shows mass to be hyperintense *(asterisks)*. Vasogenic edema in the right frontal lobe indicates direct brain invasion by the tumor.

D, Axial CT shows bowing of medial orbital walls caused by the expansile nature of the mass. Ethmoid plates and the nasal septum are destroyed.

a decrease in the amount of this enhancing tissue to exclude residual or recurrent tumor. In most cases, there was retained fluid and mucosal thickening in the paranasal sinuses and nasal vaults.

The MR scans after craniofacial resection demonstrated a variety of appearances in the space between the anterior wall of the surgically obliterated frontal sinus and the dura (Figs 1F and 2C). Most commonly there was a thin layer of tissue that was hypointense signal on T1-weighted images that enhanced and became moderately hyperintense on T2-weighted images. We presume this represents granulation tissue similar to the tissue usually present in the superior nasal cavity. Often there was an associated central fluid component that did not enhance. Occasionally there was nonenhancing tissue of high signal on T1-weighted images, which lost signal on T2-weighted images. This represented fat placed at surgery in this space. Scans obtained relatively early after craniofacial resection occasionally showed evidence of blood-breakdown products, that is, methemoglobin that was high on T1- and T2-weighted sequences.

Discussion

Esthesioneuroblastoma may arise anywhere throughout the distribution of the olfactory epithelium, which extends from the cribriform plate to the middle turbinates (1). Patients initially present with nasal symptoms, most frequently unilateral nasal obstruction and epistaxis. Other symptoms, such as rhinorrhea and anosmia, may be present. A cerebrospinal fluid leak and headache may develop (2). Often the initial clinical diagnosis is incorrect. Nasal carcinoma, nasal polyps, or sinusitis may be suspected. The differential diagnosis of a superior nasal vault mass includes squamous cell carcinoma, adenoid cystic carcinoma, sinonasal undifferentiated carcinoma, malignant melanoma, lymphoma, lymphoepithelioma, extramedullary plasmacytoma, minor salivary gland tumors, neuroma, and sarcoma (especially rhabdomyosarcoma) (3).

Esthesioneuroblastoma bears histologic resemblance to neuroblastomas at other sites. Esthesioneuroblastoma has become recognized increasingly by surgical pathologists with the clarification of the light-microscopic features and clinical awareness (4). The presence of either an intercellular fibrillary background or Homer Wright rosettes in a sinonasal neoplasm is diagnostic for esthesioneuroblastoma. Formerly, esthesioneuroblastomas were classified as neuroepitheliomas, neuroblastomas, or neurocytomas. Such designations were abandoned when subsequent data showed a lack of correlation between morphologic features and prognosis (5, 6). Occasionally, electron microscopy and immunohistochemistry studies are needed to confirm the diagnosis. Olfactory neuroblastoma is used more commonly by surgical pathologists; esthesioneuroblastoma is the most widely accepted term by head and neck surgeons (3).

The MR appearance of esthesioneuroblastoma is variable. The tumor can have homogeneous or heterogeneous signal characteristics. Compared with brain gray matter the tumors are generally hypointense on T1-weighted images and isointense to hyperintense on proton-density and T2-weighted images. We chose to compare the tumor signal intensity with gray matter, because in all cases the tumor was hyperintense to white matter and muscle on T2-weighted images. The tumors can almost always be differentiated from entrapped sinus fluid after careful scrutinization and comparison of all image sequences, including postcontrast scans. The tumors in our series did not demonstrate evidence of hemorrhage. The MR appearance of the recurrent esthesioneuroblastoma did not differ significantly from tumors imaged at initial presentation. Contrast enhancement of the tumor is variable but always present. Esthesioneuroblastoma often expands the nasal cavity, usually with concurrent destruction of the nasal septum, turbinates, and ethmoid septa. Local extension with further bone destruction can occur. Although subtle erosion of the cribriform plate and roof of the ethmoids is better seen on CT, esthesioneuroblastoma usually presents at a stage at which the cribriform plate involvement is easily seen on MR as well. It is not crucial to detect subtle involvement of the cribriform plate, because this structure is resected en bloc at the time of craniofacial resection (7). These MR features of esthesioneuroblastoma are nonspecific and cannot be differentiated readily from differential considerations listed above. Biopsy may be required to make a definitive diagnosis.

The CT features of esthesioneuroblastoma are a homogeneous soft-tissue mass with relatively uniform enhancement centered in the superior nasal cavity (8). Bone molding and erosion is frequent. Calcification has been reported in esthesioneuroblastoma both histologically and radiologically (9, 10). Som et al have pointed out that CT provides an accurate assessment of the

extent of sinonasal tumors before craniofacial resection (11). This may result in modification of the craniotomy flap size and extent of dura or brain to be removed. Another series with fewer patients examined with MR and a case report have specifically discussed the appearance of esthesioneuroblastoma on MR (12, 13). A review of the MR appearance of sinonasal sinus tumors concluded that nearly 95% of tumors in this region have intermediate signal on T2-weighted images and are generally homogeneous in appearance (14). The authors found that the remaining 5% of tumors that have increased signal are almost exclusively minor salivary-gland tumors and some neuromas. However, only 3 of the 53 tumors in this series were esthesioneuroblastomas. In our series of esthesioneuroblastoma, 53% (8 of 15) had predominately increased signal on T2-weighted images when compared with brain gray matter. However, in all cases the tumors were less intense than the very high signal of nondehydrated sinus fluid. Therefore, if a sinonasal tumor demonstrates increased signal on T2-weighted images, esthesioneuroblastoma should be considered in the differential diagnosis, but the presence of predominately intermediate signal does not exclude it. Another report concluded that malignant sinonasal tumors that invade the anterior cranial fossa tended to have a homogeneous appearance, whereas inflammatory polyps and occasional mucoceles that invaded the anterior cranial fossa had a heterogeneous MR appearance (15). However, 1 of the 2 esthesioneuroblastomas in that series did have heterogeneous signal thought to be caused by tumor necrosis. In our series, 4 of the 6 esthesioneuroblastomas that invaded the anterior cranial fossa had heterogeneous signal. However, none of these 4 cases had the very low signal of desiccated secretions, which are often associated with mucoceles and inflammatory disease (16).

We agree with others that MR is superior to CT in mapping sinonasal tumor extension because of its ability to distinguish tumor from inflammatory tissue and multiplanar imaging capability (14). In general, T2-weighted images are the most useful in distinguishing tumor from associated inflammatory disease. The proton-density images in our series did not provide any unique information. Because there is a spectrum of signal intensities that are demonstrated by chronically obstructed sinuses on T2-weighted images (17), we feel that the precontrast T1-weighted images occasionally contribute unique information to make this distinction (Figs 1D and 1E). In addition, this sequence serves as a comparison for the postcontrast T1-weighted images. Our experience in this series also supports the conclusions of Lanzieri et al that gadolinium-enhanced images can be useful in differentiating neoplasms from coexisting inflammatory disease (18). Postcontrast T1-weighted images are also the most useful in depicting the margins of intracranial extension.

In 1976, Kadish et al proposed a staging classification of esthesioneuroblastoma based on extent of disease: stage A is involvement of the nasal cavity only; stage B is involvement of the nasal cavity and one or more paranasal sinus; and stage C is involvement outside the nasal cavity including orbit, base of skull, intracranial cavity, cervical nodes, or distant metastases (19). The optimal treatment for esthesioneuroblastoma remains controversial (20). Some authors recommend radiation therapy or surgery alone for early-stage disease, reserving the alternative modality as salvage therapy for treatment failures. The current treatment policy at our institution consists of radiation therapy (50 Gy) followed 4 to 6 weeks later by surgery for stage A and B disease. For stage C disease chemotherapy consisting of cyclophosphamide and vincristine is given before radiation therapy.

MR is obtained at initial tumor presentation for staging. If a high-resolution CT scan is initially available and demonstrates no erosion through the cribriform plate or roof of the ethmoids, an MR scan may not be obtained until after preoperative radiation therapy. At this point, we feel MR is superior to CT in differentiating tumor from entrapped sinus fluid before surgery. Cervical lymph node metastases occur in 17% of cases at presentation (20). Distant disease is unusual at presentation but may occur subsequently at the time of relapse in bone, bone marrow, lung, or skin. An imaging study of the neck is obtained only if enlarged lymph nodes are found at physical examination.

The combined otolaryngologic and neurosurgical approach to the anterior skull base is the safest method to evaluate intraoperatively and resect tumors involving the roof of the nasal vault and the ethmoid complex (21, 22). Before the acceptance of this concept, local resection of esthesioneuroblastoma via lateral rhinotomy without the anterior craniotomy was associated with a high local recurrence rate because of inadequate tumor resection (23). At our institu-

tion an approach through the frontal sinus is used to obtain access to the floor of the anterior cranial fossa instead of a frontal craniotomy, which can be disfiguring because of the required burr holes (Fig 5) (24). An osteoplastic flap through the confines of the anterior wall of the sinus is made and returned at the completion of the procedure. The mucosa of the frontal sinus is removed, and this space is packed with pericranium, fibrin glue, Scarpa's fascia and fat, and split-thickness skin graft. The extent of exposure includes the midline of the anterior cranial fossa and the medial orbital roofs, to the tuberculum of the sella turcica. The exposure can be extended laterally or posteriorly to the orbital apex. The anterior cranial base defect is closed by a periosteal flap based anteriorly on the supraorbital and supratrochlear vessels. After dural closure, the first layer of closure is the pericranial flap. Wire or fixation plates are used to secure the anterior wall of the frontal sinus. A lateral rhinotomy or facial degloving technique is used for the facial portion of the resection. Depending on each specific tumor's location, the cribriform plate, nasal septum, ethmoid complex, turbinates, and included portions of the maxillary and/or sphenoid sinus are removed.

Potential complications of this procedure include postoperative cerebrospinal fluid leaks, symptomatic pneumocephalus, epidural hematoma, bone flap infection, and epidural abscess. The 2-year determinate survival rate of patients with esthesioneuroblastoma is 88%, compared with 50% in the era before craniofacial resection, suggesting an improvement in local control with more aggressive initial therapy (25). Most recurrences present within the first 2 years, with the longest disease-free interval before recurrence being almost 8 years after definitive treatment. Therefore, MR is usually obtained approximately 3 months after the initial procedure to serve as a baseline. Follow-up MR exams are obtained at 6-month intervals for 3 years, followed by yearly examinations for at least 5 years.

MR scans after craniofacial resection usually demonstrate enhancing soft tissue at the resection site in the superior nasal cavity that often cannot be differentiated from residual or recurrent tumor. The difficulty in differentiating mature granulation tissue and tumor in a postoperative patient by MR has been previously recognized (14). The close follow-up with MR is required to assess for interval change that would require biopsy. Som et al discussed the postoperative CT appearance after craniofacial resection (11). The changes in the calvarium are better appreciated on CT. However, we feel MR to be better than CT in evaluating the high nasal cavity after craniofacial resection because of its superior ability to differentiate soft tissue, which could represent recurrent tumor, from fluid, fat, and the fascial and muscular support flaps placed at surgery.

Although the MR features of esthesioneuroblastoma are not specific, this malignancy should be considered when a mass in the superior nasal cavity is identified that demonstrates both expansile and destructive characteristics and erodes the cribriform plate or roof of the frontoethmoid complex. MR is our imaging modality of choice for depicting tumor extension, which is critical for staging and evaluating for recurrence after craniofacial resection.

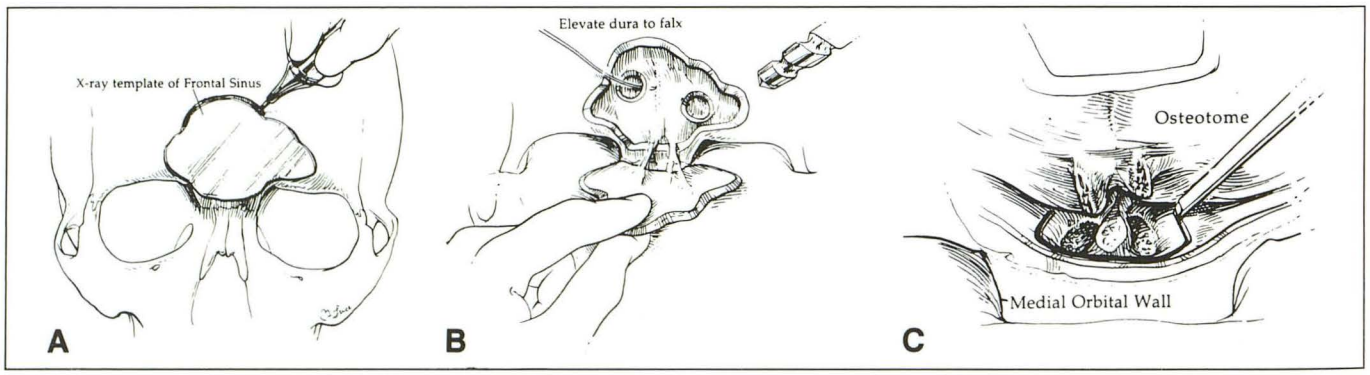

Fig. 5. Intraoperative drawings, modified from Persing et al (24).

A, The frontal sinus perimeter osteotomy is planned using an x-ray template.

B, The anterior wall of the frontal sinus is lifted forward, exposing the posterior sinus wall for burr-hole placement through which the dura can be elevated.

C, The posterior wall of the frontal sinus and the crista galli are removed to aid visualization of the olfactory fiber-associated dura. An osteotomy is performed under direct visualization.

References

1. Nakashima T, Kimmelman CP, Snow JB. Structure of human fetal and adult olfactory neuroepithelium. *Arch Otolaryngol Head Neck Surg* 1984;110:641–646
2. Cantrell R, Ghorayeb BY, Fitz-Hugh GS. Esthesioneuroblastoma: diagnosis and treatment. *Ann Otol Rhinol Laryngol* 1977;86:760–765
3. Stewart FM, Frierson HF, Levine PA, Spaulding CA. Esthesioneuroblastoma. In: Williams CJ, Krikorian JC, Green MR, Raghavan D, eds. *Textbook of uncommon cancer.* New York: Wiley, 1988;631–652
4. Newbill ET, Johns ME, Cantrell RW. Esthesioneuroblastoma: diagnosis and management. *South Med J* 1985;78:275–282
5. Mills SE, Frierson HF. Olfactory neuroblastoma. *Am J Surg Pathol* 1985;9:317–327
6. Oberman HA, Rice DH. Olfactory neuroblastomas. *Cancer* 1976;38:2494–2502
7. Levine PA. Craniofacial resection for tumors of the ethmoid and superior nasal vault. In: Jacobs C, ed. *Carcinomas of the head and neck: Evaluation and management.* Boston: Klower, 1990;47–53
8. Hurst RW, Erickson S, Cail WS, et al. Computed tomographic features of esthesioneuroblastoma. *Neuroradiology* 1989;31:253–257
9. Manelfe C, Bonafe A, Fabre P, Pessey JJ. Computed tomography in olfactory neuroblastoma: one case of esthesioneuropithelioma and four cases of esthesioneuroblastoma. *J Comput Tomogr* 1978;2:412–420
10. Regenbogen VS, Zinreich SJ, Kim KS, et al. Hyperostotic esthesioneuroblastoma: CT and MR findings. *J Comput Assist Tomogr* 1988;12:52–56
11. Som PM, Lawson W, Biller HF, Lanzieri CF, Sachdev VP, Rigamonti D. Ethmoid sinus disease: CT evaluation in 400 cases, III: craniofacial resection. *Radiology* 1986;159:605–609
12. Woodhead PA, Lloyd GA. Olfactory neuroblastoma: imaging by magnetic resonance, CT, and conventional techniques. *Clin Otolaryngol* 1988;13:387–394
13. Schroth G, Grawehn J, Marquardt B, Schabet M. MR imaging of esthesioneuroblastoma: case report. *J Comput Assist Tomogr* 1986;10:316–319
14. Som PM, Shapiro MD, Biller F, Sasaki C, Lawson W. Sinonasal tumors and inflammatory tissues: differentiation with MR imaging. *Radiology* 1988;167:803–808
15. Som PM, Dillon WP, Sze G, Lidov M, Biller HF, Lawson W. Benign and malignant sinonasal lesions with intracranial extension: differentiation with MR imaging. *Radiology* 1989;172:763–766
16. Van Tassel P, Lee YY, Jing BS, et al. Mucoceles of the paranasal sinuses: MR imaging with CT correlation. *AJNR Am J Neuroradiol* 1989;10:607–612
17. Som PM, Dillon WP, Fullerton GD, Zimmerman RA, Rajagopalan B, Marom Z. Chronically obstructed sinonasal secretions: observations on T1 and T2 shortening. *Radiology* 1989;172:515–520
18. Lanzieri CF, Shah M, Krauss D, Lavertu P. Use of gadolinium-enhanced MR imaging for differentiating mucoceles from neoplasms in the paranasal sinuses. *Radiology* 1991;178:425–428
19. Kadish S, Goodman M, Warg CC. Olfactory neuroblastoma. *Cancer* 1976;37:1571–1576
20. Spaulding CA, Kronyak MS, Constable WC, Stewart FM. Esthesioneuroblastoma: a comparison of two treatment era. *Int J Radiat Oncol Biol Phys* 1988;15:581–590
21. Levine PA, Scher RL, Jane JA, et al. The craniofacial resection-eleven year experience at the University of Virginia: problems and solutions. *Otolaryngol Head Neck Surg* 1989;101:665–669
22. Cheesman AD, Lund VJ, Howard DJ. Craniofacial resection for tumors of the nasal cavity and paranasal sinuses. *Head Neck Surg* 1986;8:429–435
23. Elner A, Koch A. Combined radiological and surgical therapy of cancer of the ethmoid. *Acta Otolaryngol (Stockh)* 1974;78:270–276
24. Persing JA, Jane JA, Levine PA, Cantrell RW. The versatile frontal sinus approach to the floor of the anterior cranial fossa. *J Neurosurg* 1990;72:513–516
25. Levine PA, McClean WC, Cantrell RW. Esthesioneuroblastoma: the University of Virginia experience 1960–1985. *Laryngoscope* 1986;96:742–746